Investigating on Wideband Phase-Modulation to Amplitude-Modulation Conversion Based on Chromatic Dispersion in Fiber

Ya Jin, Yinfang Chen, Zhuang Xie, Changda Xu, Huatao Zhu, and Ninghua Zhu, *Member, IEEE*

***Abstract*—We investigate on the wideband phase-modulation to amplitude-modulation (PM-AM) conversion based on the chromatic dispersion in fiber. To overcome the shortcomings of the single-tone or dual-tone modulation-based model in previous researches, we present a more intuitive time-frequency analysis method for the propagation of phase-modulated signals in dispersive fibers, and give the physical picture for the temporal waveform changes. By analyzing the amplitude variation near the transition zone, we establish a bit-by-bit correspondence between the pulse waveforms and the actual modulated data, and realized the non-return-to-zero (NRZ) differential phase-shift keying (DPSK) demodulation. Furthermore, the effect of fiber length and bit rate on PM-AM conversion is also investigated quantitatively and experimentally.**

***Index Terms*—Phase-modulation to amplitude-modulation conversion, NRZ DPSK demodulation, chromatic dispersion.**

I. Introduction

OVER the past few decades, the microwave photonics (MWP), where the generating, manipulating, transporting and measuring of high-speed radio-frequency (RF) signals are transferred to the optical frequency for processing, has attracted great attention from worldwide researchers [1]–[3]. Phase modulator, as a key optical device, has been widely used in MWP systems due to its simple structure and no bias drifting compared to Mach–Zehnder modulators (MZM) [4]. In theory, the envelope of phase-modulated signals keeps a constant, and cannot be directly detected by a photodetector (PD). However, due to the propagation impairments in MWP links, the phase modulation would partly convert into amplitude modulation. Although this may cause adverse effects such as power overshoot, signal distortion, etc., PM-AM conversion has still found many important applications in microwave photonic filters [5], [6], optoelectronic oscillators [7], [8] and so on.

There are many comprehensive studies on the causes of the phase modulation to amplitude modulation conversion (PM-AM conversion), including gain filtering, chromatic dispersion as well as frequency conversion [9]. Exploiting the dispersion effect in the fiber is one of these conversion methods, which is natural and practical that does not require additional components. However, most reported researches have adopted analytical models based on sinusoidal microwave signals, which can only be applied to simple scenarios of single-tone transmission or dual-tone transmission, and an intuitive description of the physical picture behind the PM-AM conversion is lacking [4], [10]–[12]. Also, bit rate error performance analysis showed that the PM-AM conversion-based receiver is similar to the on-off keying receiver with sufficient dispersion, but the waveform change in PM-AM conversion has not been considered [13]. In this sense, a more intuitive time-frequency analysis method for PM-AM conversion is required. In addition, few studies have attempted to apply PM-AM conversion research to phase modulation based fiber-optic communication systems.

In this paper, we investigate the wideband PM-AM conversion based on the chromatic dispersion in the fiber, and realize the novel detection for non-return-to-zero (NRZ) DPSK signals without delay interferometer or balanced receivers. To better explain the PM-AM conversion in the dispersive fiber, a more intuitive time-frequency analysis method corresponding to square-wave modulating signal is established. We successfully demonstrate a proof-of-concept experiment on DPSK signal demodulation over a 25 km single-mode fiber (SMF) span. Moreover, the effect of the fiber lengths and the bit rate on the temporal waveforms is experimentally investigated.

II. Operation Principles

Consider a transmission link composed of a phase modulator (PM), a span of SMF and a photodetector (PD). As shown in Fig. 1, the phase-modulated signal, after transmission via fiber, is sent to the PD for direct detection.

Manuscript received 8 July 2022; accepted 3 August 2022. Date of publication 8 August 2022; date of current version 17 August 2022. This work was supported in part by the National Natural Science Foundation of China under Grant 61901480 and in part by the National Key Research and Development Program of China under Grants 2020YFF0400602 and 2019YFB2205302. *(Corresponding author: Huatao Zhu.)*

Ya Jin and Changda Xu are with the State Key Laboratory of Integrated Optoelectronics, Institute of Semiconductors, Chinese Academy of Sciences, Beijing 100083, China, and also with the University of Chinese Academy of Sciences, Beijing 100049, China (e-mail: jinya@semi.ac.cn; xuchangda18@semi.ac.cn).

Yinfang Chen and Ninghua Zhu are with the State Key Laboratory of Integrated Optoelectronics, Institute of Semiconductors, Chinese Academy of Sciences, Beijing 100083, China (e-mail: yfchen17@semi.ac.cn; nhzhu@semi.ac.cn).

Zhuang Xie is with the Xi'an Institute of Optics and Precision Mechanics, Chinese Academy of Sciences, Xi'an 710119, China, and also with the University of Chinese Academy of Sciences, Beijing 100049, China (e-mail: xiezhuang@opt.ac.cn).

Huatao Zhu is with the College of Information and Communication, National University of Defense Technology, Wuhan 430010, China (e-mail: zhuhuatao2008@163.com).

Digital Object Identifier 10.1109/JPHOT.2022.3197209

This work is licensed under a Creative Commons Attribution 4.0 License. For more information, see https://creativecommons.org/licenses/by/4.0/

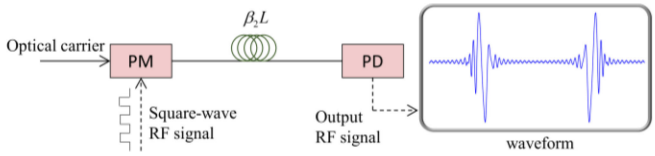

Fig. 1. Diagram of phase-modulated MWP links with dispersion fiber. PM: phase modulator, SMF: single-mode fiber, PD: photodetector, RF: radio frequency.

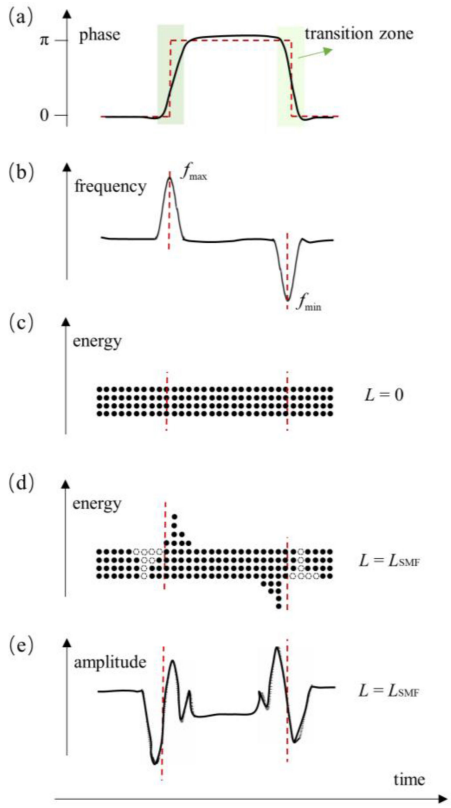

Fig. 2. Schematic diagram of the conversion of PM-AM due to chromatic dispersion. (a) Transition zone in DPSK signal. (b) Chirp in the transition zone. (c)(d) The redistribution of energy in time through fiber transmission over a distance. (e) Corresponding amplitude variation.

The phase-modulated optical signal can be written as

$$E_0(t) \propto \exp\left(jmg\left(t\right)\right), \tag{1}$$

where m is the modulation index, and $g(t)$ is the modulated signal.

Ignoring the fiber-induced attenuation and high-order dispersion, the transfer function of the dispersive fiber with a length L can be expressed as [14], [15]

$$H(j\omega) = \exp\left(\frac{1}{2}j\beta_2 L\omega^2\right), \tag{2}$$

where β_2 is the second-order dispersion coefficient of the optical fiber, ω is the offset angular frequency relative to the carrier.

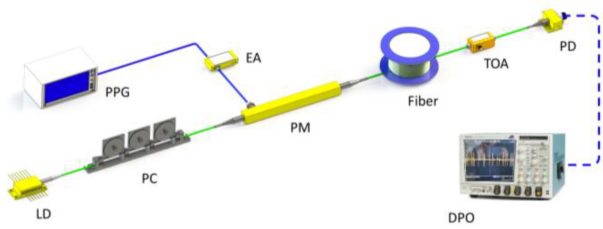

Fig. 3. Experimental setup of the DPSK demodulation based on the wideband PM-AM conversion. LD: laser diode, PC: polarization controller, PM: phase modulator, EA: electric amplifier, PPG: pseudo-random pulse generator, TOA: tunable optical attenuator, PD: photodetector, DPO: digital phosphor oscilloscope.

After the phase-modulated signal passes through the SMF, we have

$$\begin{aligned} E_d(t) &= E_0(t) \otimes \left[\frac{1}{2\pi}\int_{-\infty}^{+\infty} H(j\omega)\cdot\exp(-j\omega t)d\omega\right] \\ &= E_0(t) \otimes \left[\frac{1}{2\pi}\int_{-\infty}^{+\infty} \exp\left(\frac{1}{2}j\beta_2 L\omega^2\right)\cdot\exp(-j\omega t)d\omega\right], \end{aligned} \tag{3}$$

where $\otimes$ denotes convolution, L is the fiber length, and the second term represents the inverse Fourier transform of fiber transfer function $\mathcal{F}^{-1}\{H(j\omega)\}$. In practice, considering the low-pass characteristics of the oscilloscope and the non-ideality of the driving signal, the NRZ square wave signal can be equivalently characterized by the Taylor expansion series of finite terms. We numerically analyzed the convolution of $E_0(t)$ and $\mathcal{F}^{-1}\{H(j\omega)\}$ in (3), and the simulation results present a waveform similar to an ultra-wideband triplet signal [16], which can be seen in the inset of Fig. 1. In other words, this triplet-like signal can represent the transition characteristics of the modulated square wave signal between bits 0 and 1. Therefore, based on the PM-AM conversion, the direct detection of the DPSK signal can actually be equivalent to detecting this triplet-like signal in the time domain.

In addition to the above mathematical expressions, we can also understand the PM-AM conversion more intuitively from the physical picture based on time-frequency analysis. Limited by the imperfect driving square wave and the response characteristics of the phase modulator itself, the DPSK signal has a transition zone with a short duration at the sudden change of phase, and the frequency in the transition zone will appear obvious changes (chirp), as shown in Fig. 2(a), (b). Due to the chromatic dispersion (corresponding to $H(j\omega)$ in (2)) the light waves of different frequencies have different group velocities in the fiber. For the SMF with quartz glass material as the main component, the higher the frequency of the transmitted light wave, the higher the refractive index of the medium, and the lower the corresponding group velocity. Taking the transition zone where the phase changes from 0 to π in Fig. 2(a) as an example, the frequency at the center is the highest (marked by the red dotted line on the left of Fig. 2(b)), that is, the light wave at $f_{\max}$ propagates more slowly compared to nearby frequencies. Then, after a certain distance through the optical fiber, the originally phase-lag light wave will catch up or even

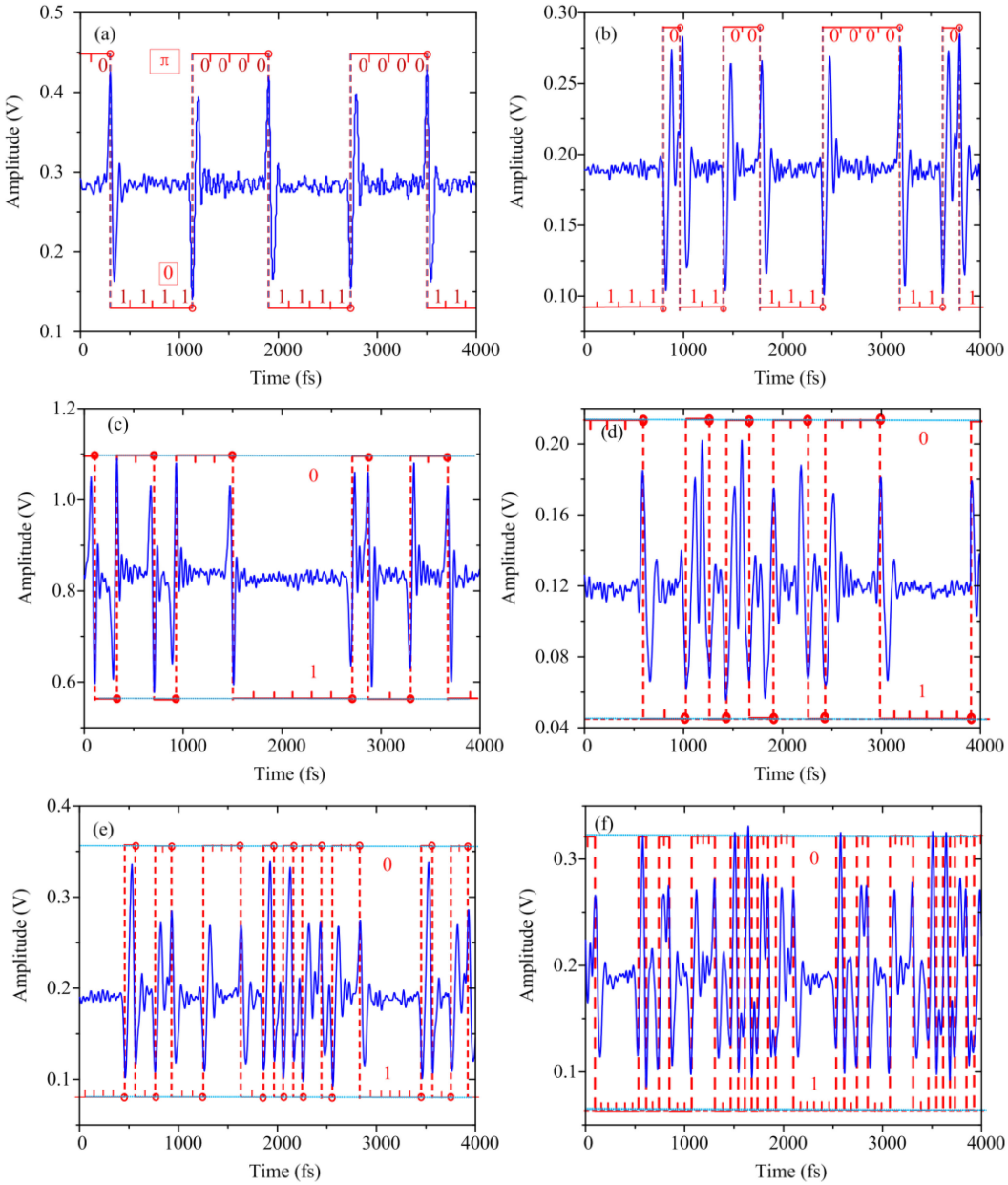

Fig. 4. Waveform analysis (a) $R = 5$ Gbps, $L = 25$ km, cyclic code [1111 0000] and demodulation results for cyclic code [1111 1011 0011 1000 0110 1010 0100 01] verification under different test conditions (b) $R = 5$ Gbps, $L = 25$ km; (c) $R = 5$ Gbps, $L = 10$ km; (d) $R = 5$ Gbps, $L = 50$ km; (e) $R = 10$ Gbps, $L = 25$ km; (f) $R = 15$ Gbps, $L = 25$ km.

exceed the light wave at $f_{\max}$, so that part of the energy on the left side of the $f_{\max}$ transitions to the right side. As depicted in Fig. 2(c), (d), as we change the phase from π to 0 (corresponding to the transition zone near $f_{\min}$), the situation is just reversed. Ultimately, the redistribution of energy near the transition zone is reflected in the amplitude variation presented as a triplet-like signal, which can be seen in Fig. 2(e).

III. Experimental Setup

The experimental setup of the demodulating the DPSK signals based on the wideband PM-AM conversion is shown in Fig. 3. The light emitted by a continuous-wave laser (LD) with a center wavelength of 1550 nm passes through a polarization controller (PC), and then is directly sent to a lithium niobate phase modulator (EOSPACE PM-DV5-40-PFA-PFA-LV) for DPSK modulation. In principle, the amplitude of the DPSK signal directly output by the PM remains constant. But after a span of SMF transmission, as the chromatic dispersions accumulate, the amplitude of the DPSK signal will change at the point where the phase abruptly changes to generate a pulse. This specific change can be obtained by acquiring and analyzing the data recorded in the digital oscilloscope (Tektronix DPO 73304D Digital Phosphor Oscilloscope) after photoelectric conversion of the signal by a square-law photodetector (PD). The sampling rate of the oscilloscope determines the fineness of the acquired

TABLE I
EXPERIMENTAL PARAMETER SETTINGS OF PROPOSED METHOD

	Waveform Analysis		Experimental verification
Cyclic codes	1111 0000	1100011 1100000	1111 1011 0011 1000 0110 1010 0100 01
Transmission rate *R* (Gbps)	2.5/5.0/7.5/10/12.5/15		
SMF lengths *L* (km)	5/10/25/50/100		

waveform. Different from the traditional demodulation scheme based on delay interferometer, the proposed scheme does not require a time delay controller for the detection of various bit rate signals, but need a higher sampling rate than traditional demodulation methods under the same bit rate. To obtain as much information as possible about the amplitude change of the triplet-like signal, we set the sampling rate to 100GS/s in the experiment. It should be noted that since the amplitude of the square wave signal output by the pseudo-random pulse generator (PPG) is generally on the order of mV, it needs to be amplified by an electric amplifier (EA) to reach the half-wave voltage of the order of V required by the PM. In addition, since the PD has a limit on the maximum input optical power, a tunable optical attenuator (TOA) needs to be connected for real-time control.

IV. RESULTS AND DISCUSSIONS

The procedure for demodulating the DPSK signals based on the wideband PM-AM conversion is as follows. First, we deliberately set two cyclic codes of "11110000" and "11000111100000" to generate the corresponding square wave signal as the radio frequency (RF) modulation signal of the PM, as shown in Fig. 4(a). By adjusting transmission rates and SMF lengths, we can analyze the corresponding triplet-like signal, or more specifically, the pulse shapes when the phase of the light wave changes rapidly between 0 and π, and the more detailed experimental parameter settings are listed in Table I. Significantly, the transmission rate provides a time scale reference for pulse analysis, while the fiber length determines the basic characteristics of the pulse, which will be analyzed in detail later. Second, we have verified the cyclic code of "1111 1011 0011 1000 0110 1010 0100 01" based on the pulse shape determined in the previous step and the corresponding transmission rate, and the demodulation results are shown in Fig. 4(b)∼(f). Closer inspection shows that the duration of bit 0 or 1 can be analyzed by the position of the different pulse peak points (marked by red circles in Fig. 4), combined with the known transmission rate, the number of bits between adjacent peak points can be determined. Furthermore, with the increase of the communication rate, when it exceeds 15 Gbps, the pulse where the bit 0 and 1 appear alternately will be difficult to maintain the shape in Fig. 4(a) because of the inter-symbol interference (ISI), which increases the difficulty of demodulation. Nevertheless, the ability to analyze pulse waveforms at higher rates or in a more complex modulation format may be enhanced in future studies by introducing emerging feature recognition technologies based on artificial intelligence.

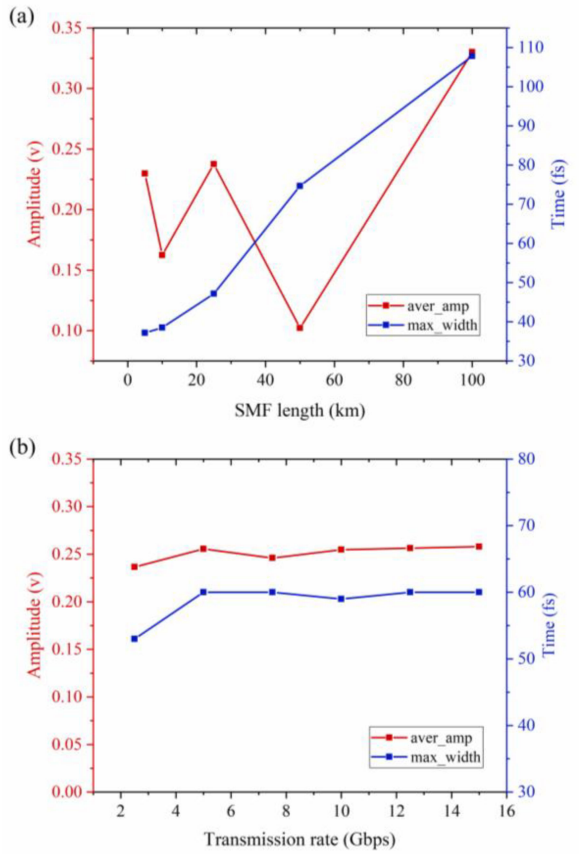

Fig. 5. Pulse analysis for different (a) SMF lengths and (b) transmission rates.

As previously described, the key to demodulating the DPSK signals based on the wideband PM-AM conversion lies in the analysis of the triplet-like signal generated near the transition zone due to chromatic dispersions. Thus, we investigated the impacts of various fiber lengths and different transmission rates on the DPSK signal, and we deliberately selected the DPSK signal modulated by the square wave RF signal corresponding to the "11110000" cyclic codes as the object of pulse analysis. We acquired temporal waveforms within 10 ns under different conditions as listed in Table I, and measured the amplitudes and widths of all pulses. We analyzed the pulse amplitudes corresponding to the maximum and minimum points near the transition zone with phase abrupt changes and the duration (pulse width) between them, and used the average pulse amplitude and maximum pulse width within these 10 ns as the characteristic quantities for analyzing amplitude changes. The test results for these two feature quantities are shown in Fig. 5. In Fig. 5(a), we can see that the average pulse amplitude has no obvious linear relationship with the length of the SMF, while the maximum pulse width is positively related to the fiber length. In other words, the longer the fiber, the more widely the energy is distributed in the time domain near the transition zone, but there is no obvious correspondence with the peak of the energy. As can be seen from Fig. 5(b), under the condition that the transmission rate R does not exceed 15 Gbps, the change of the R has little effect on the average pulse amplitude and maximum pulse width.

It is worth mentioning that if we adopt "0101" cyclic codes, an increase in R can adversely affect the quantitative analysis of pulse waveform due to ISI. In addition, since there is a transition zone with abrupt phase change in any PSK signal, the scheme we propose also has good adaptability for more complex modulation formats embedding PSK modulation. In particular, based on the wideband PM-AM conversion induced waveform changes in the fiber we investigated, besides applying to the demodulation of DPSK signals, it has great potential applications in many fields such as the identification of optical signals, optical network performance monitoring, target detection and imaging and so on.

V. Conclusion

In summary, the wideband PM-AM conversion based on the chromatic dispersion in fiber has been investigated, and a more intuitive time-frequency analysis method with clear physical picture is proposed. Based on the proposed model, we demonstrated a novel detection method for DPSK signal with a simple structure through a proof-of-concept experiment. The experimental results show that by analyzing the triplet-like signal generated near the transition zone, the DPSK signal up to 15 Gbps can be correctly demodulated with the PM-AM conversion in the fiber. In addition, the temporal waveform is affected by system parameters, such as bit rate, fiber length. Overall, this work has provided a deeper insight into the PM-AM conversion in the fiber, and may be widely applied in the fields of optical communications and sensing.

Acknowledgment

The authors wish to thank the anonymous reviewers for their careful reading and valuable suggestions and declare no conflicts of interest.

References

[1] J. Yao, "Microwave photonic sensors," *J. Lightw. Technol.*, vol. 39, no. 12, pp. 3626–3637, Jun. 2021, doi: 10.1109/JLT.2020.3047442.

[2] D. Marpaung, J. Yao, and J. Capmany, "Integrated microwave photonics," *Nature Photon.*, vol. 13, no. 2, pp. 80–90, Feb. 2019, doi: 10.1038/s41566-018-0310-5.

[3] V. J. Urick, J. D. Mckinney, and K. J. Williams, *Fundamentals of Microwave Photonics: Urick/Fundamentals of Microwave Photonics*. Hoboken, NJ, USA: Wiley, 2015, doi: 10.1002/9781119029816.

[4] H. Chi, X. Zou, and J. Yao, "Analytical models for phase-modulation-based microwave photonic systems with phase modulation to intensity modulation conversion using a dispersive device," *J. Lightw. Technol.*, vol. 27, no. 5, pp. 511–521, Mar. 2009, doi: 10.1109/JLT.2008.2004595.

[5] O. Daulay, G. Liu, and D. Marpaung, "Microwave photonic notch filter with integrated phase-to-intensity modulation transformation and optical carrier suppression," *Opt. Lett.*, vol. 46, no. 3, Feb. 2021, Art. no. 488, doi: 10.1364/OL.413579.

[6] Z. Zeng et al., "Freely tunable dual-passband microwave photonic filter based on phase-to-intensity modulation conversion by stimulated Brillouin scattering," *IEEE Photon. J.*, vol. 11, no. 1, Feb. 2019, Art. no. 5501009, doi: 10.1109/JPHOT.2019.2897593.

[7] J. Zhang, Y. Wang, X. Li, Z. Liu, and J. Wo, "Tunable multi-frequency optoelectronic oscillator based on a microwave photonic filter and an electrical filter," *Opt. Quant. Electron.*, vol. 53, no. 7, Jul. 2021, Art. no. 407, doi: 10.1007/s11082-021-03061-0.

[8] T. Hao, J. Tang, N. Shi, W. Li, N. Zhu, and M. Li, "Dual-chirp Fourier domain mode-locked optoelectronic oscillator," *Opt. Lett.*, vol. 44, no. 8, Apr. 2019, Art. no. 1912, doi: 10.1364/OL.44.001912.

[9] J. Yao, "Photonics to the rescue: A fresh look at microwave photonic filters," *IEEE Microw. Mag.*, vol. 16, no. 8, pp. 46–60, Sep. 2015, doi: 10.1109/MMM.2015.2441594.

[10] A. R. Charaplyvy, R. W. Tkach, L. L. Buhl, and R. C. Alferness, "Phase modulation to amplitude modulation conversion of CW laser light in optical fibres," *Electron. Lett.*, vol. 22, no. 8, 1986, Art. no. 409, doi: 10.1049/el:19860279.

[11] J. F. Diehl and V. J. Urick, "Chromatic dispersion induced second-order distortion in long-haul photonic links," *J. Lightw. Technol.*, vol. 34, no. 20, pp. 4646–4651, Oct. 2016, doi: 10.1109/JLT.2016.2552080.

[12] T. Yamamoto, T. Mori, T. Sakamoto, K. Kurokawa, S. Tomita, and M. Tsubokawa, "Group velocity dispersion measurement method using sinusoidally phase-modulated continuous wave light based on cyclic nature of optical waveform change by group velocity dispersion," *Appl. Opt.*, vol. 49, no. 27, Sep. 2010, Art. no. 5148, doi: 10.1364/AO.49.005148.

[13] M. Franceschini, G. Bongiorni, G. Ferrari, and R. Raheli, "Direct-detection optical DPSK," in *Proc. Conf. Opt. Fiber Commun./Nat. Fiber Optic Engineers Conf.*, Feb. 2008, pp. 1–3. doi: 10.1109/OFC.2008.4528777.

[14] Y. Zhu, X. Miao, Q. Wu, L. Yin, and W. Hu, "Imbalanced Mach-Zehnder modulator for fading suppression in dispersion-uncompensated direct detection system," *Electronics*, vol. 10, no. 22, Nov. 2021, Art. no. 2866, doi: 10.3390/electronics10222866.

[15] G. P. Agrawal, *Nonlinear Fiber Optics*, 6th ed., London, U.K.: Academic, 2019.

[16] M. Rius, M. Bolea, J. Mora, and J. Capmany, "High-order UWB pulses generation adaptable to bi-phase modulation," *IEEE Photon. Technol. Lett.*, vol. 28, no. 21, pp. 2371–2374, Nov. 2016, doi: 10.1109/LPT.2016.2594154.